NONLINEAR DYNAMICS OF A SEGMENTED SKIRT AIR CUSHION

T. A. GRAHAM and P. A. SULLIVAN

Institute for Aerospace Studies
University of Toronto
Toronto, Canada

ABSTRACT

This paper gives results from a simulation of the pitch-heave dynamics of an uncompartmented segmented skirt air cushion vehicle. The simulation includes nonlinearities associated with skirt-ground contact. As modelled, the system consists of a ducted fan discharging into a plenum chamber. Results from several system models are presented and compared for a laboratory vehicle. System models of fourth and sixth order are developed; a quasisteady fan characteristic is used and the sixth order model includes additional orders for a lumped inertance model of the ducting and a pneumatic capacitance model of the cushion. The skirt is assumed to be a massless membrane capable of supporting some force in compression and to deform according to a geometric theory on contact with the ground. Three different geometric theories are compared through their effects on vehicle statics and dynamics. Large variations are found for some of the system response parameters, for example, the pitch stiffness. Predictions of pitch stiffness and footprint area are compared with static data. Predictions for a large scale craft indicate significant dynamic effects resulting from the capacitance and inertance.

INTRODUCTION

One of the objectives of the Air Cushion Vehicle (ACV) research program at the University of Toronto Institute for Aerospace Studies (UTIAS) is to study the dynamics of ACV's equipped with the uncompartmented segmented skirt system shown in figure 1. This skirt has been used in icebreaking, low speed barge, and ferry applications. Typical craft using this skirt are the air cushion icebreaking bow (ACIB), the Hoverlift Systems HL101, and the Air Trek 140. Initial UTIAS studies of this skirt resulted in an experimentally validated theory for the pitch and roll stiffness of this skirt system which was presented in reference 1. This theory has been extended and incorporated into a dynamics model. This paper presents some preliminary results from this model.

A dynamic theory for the cushion must describe the method of generating restoring forces, predict cushion pressure and flow, and model the vehicle motion. The restoring forces, cushion pressure and centre of gravity motion are intrinsically coupled. For example, in order to apply Newton's laws of mechanics, the movement of the centre of mass that occurs during a pitching manoeuvre must be known to reasonable accuracy. Also, application of the basic cushion mass flux conservation law requires information about the mass flux of air from the cushion. This must be calculated and requires knowledge of both the cushion pressure and the effective air escape area generated by the cushion as a result of its motion. Thus, as a minimum, the air escape area geometry during motion and a description of the duct-fan flow characteristics are necessary.

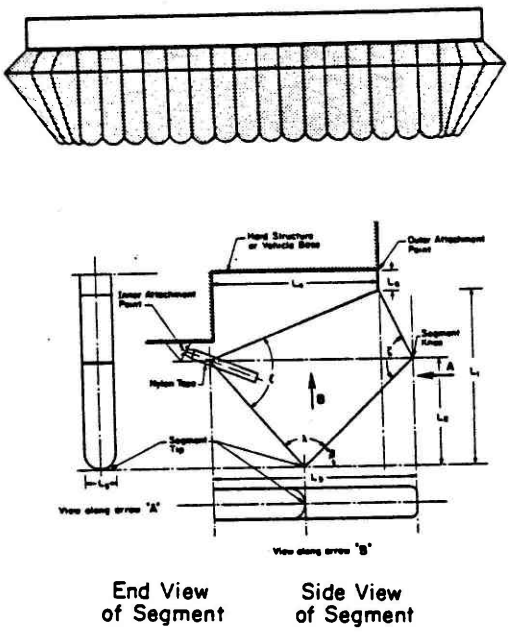

FIGURE 1: Segmented Skirt System

Force and moment measurements made on full scale and laboratory vehicles have shown that static hysteresis can exist in the heave stiffness [1] and pitch stiffness [2] curves, see figure 2.

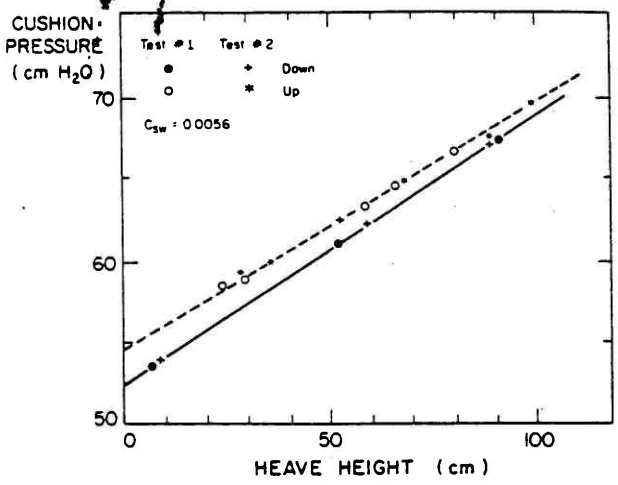

FIGURE 2: Experimental Data Showing Hysteresis in Heave Cycle Tests on the Air Cushion Icebreaker Bow (ACIB)

This hysteresis represents damping in the dynamics and tests on the UTIAS circular track vehicle [3] indicate that all the static hysteresis contributes to the vehicle's damping. Although studies are currently in progress at UTIAS the nature and cause of this hysteresis is not adequately understood. The forces are, however, generated during skirt ground contact and current thinking is that they arise from local buckling which occurs as a result of this contact.

The geometry of an amphibious air cushion skirt system also plays an important role in determining the system stiffness and damping parameters. Some systems, such as the British Hovercraft (BHC) bag and finger skirt, the Bertin multicell, and the peripheral cell cushion achieve pitch and roll stiffness primarily through cushion compartmentation; others such as the Hovercraft Development Ltd. (HDL) loop and segment skirt allow the skirt to shift laterally relative to the vehicle centre of mass to obtain pitch and roll stiffness. The uncompartmented segmented skirt system differs from these in that it obtains pitch and roll stiffness through centre of pressure shifts resulting only from the deformation of the skirt which occurs during surface contact. The details of the contact area are thus crucial for a good qualitative and quantitative study of segmented skirt system dynamics. Several approximations to the footprint geometry are presented here to demonstrate its effect on predicted cushion response.

The duct-fan flow model for the system requires the both steady fan characteristic and terms to account for dynamic effects When the blade aerodynamics are steady, the fan and duct dynamics be handled by the method of characteristics [2,4], transmission line techniques [2,4], or a lumped parameter model, depending on the accuracy required, the system geometry, and the frequency range of interest. For the laboratory craft under study frequencies of vehicle dominated motion are low and dimensions are small enough so that the lumped parameter model assumptions are valid. Therfore a lumped parameter approach which utilizes an inertance for the duct and a capacitance for the plenum, has been chosen for this investigation.

The lumped parameter models permit direct comparison of different system models. Thus it can be determined if the added inertance and capacitive orders represent significant differences in vehicle response. It has been shown by Sweet, Richardson,and Wormley [5] that inclusion of capacitance is required to predict dynamic heave stability. Hinchey [6] has shown that even relatively short duct feeding systems can radically shift heave stability boundaries. Captain, Boghani, et al [7] have also indicated that duct inertia and plenum capacitance are of fundamental importance for air cushion response prediction. Doctors has shown [8] that at higher frequencies the cushion capacitance represents large deviations in response amplitude and phase characteristics. However, many authors ignore the capacitance citing reasons such as "likely to be less important at lower frequencies" [9], or "Because of the large leakage of ACV's the effects of compressibility and hence absolute pressure may be neglected" [10]. Simply put, criteria for the inclusion of orders for capacitance and/or inductance have not been adequately delineated so that a complete dynamics investigation should assess the effects of both.

EQUATIONS OF MOTION

The equations of pitch-heave motion include Newton's law for the heave motion, Euler's equation for pitch motion, the lumped capacitance equation for the combined plenum box cushion volume, and the lumped inertance equation for the fan-duct system. The resulting sixth order dynamics mode is based on the following assumptions:

i) the vehicle is moving at zero forward speed and is disturbed in pitch and heave only.

ii) gyroscopic effects from rotating subassemblies such as fans and propellers are negligible.

iii) the skirt system is massless and inelastic and deforms according to a geometric theory on contact with the ground.

iv) the skirt material damping forces can be represented by a static hysteresis model where forces are proportional to the perimeter of skirt in contact. These skirt forces act only when the material is being compressed, that is that no force acts when the amount of compression is being reduced.

v) the frequencies of excitation and oscillation are low enough that the lumped parameter models apply to the flow

processes. A conservative empirical criterion for this is that

$$f < 0.04a/L \qquad (1)$$

where a is the speed of sound and L is the longest dimension of the flow element, [4].

vi) the fan blade aerodynamics are quasi-steady.

vii) cushion exhaust flow is governed by the quasisteady orifice flow law.

viii) vehicle motion is about the centre of mass which lies on the longitudinal and lateral axes of symmetry of the craft.

ix) ground friction is negligible.

x) cushion internal flow effects are small.

The resulting system equations are given as follows:

The heave force balance:

$$m\ddot{h} = p_c a_f(h,\theta) - mg + H_h(h,\theta,\dot{h},\dot{\theta}) \qquad (2)$$

where m is the cushion mass
h is the cushion centre of mass height above datum
θ is the pitch angle
p_c is the cushion plenum pressure
a_f is the cushion footprint area
g is gravitational acceleration
H_h is the magnitude of the heave hysteresis force
and $\dot{(\ )}$ is dot notation for time derivatives => $d(\ )/dt$.

The pitch moment balance:

$$I_{yy}\ddot{\theta} = M_p(h,\theta,p_c) + H_p(h,\theta,\dot{h},\dot{\theta}) \qquad (3)$$

where I_{yy} is the pitch moment of inertia,
M_p is the cushion restoring moment given by

$$M_p = -p_c a_f(h,\theta)\bar{x}(h,\theta) + M_{pf}(h,\theta,p_c), \qquad (4)$$

$\bar{x}$ is the moment of the centre of pressure from the centre of mass,
M_{pf} is a minor contribution due to momentum of fluid exiting from the cushion,
and H_p is the pitch hysteresis term.

Conservation of mass for the cushion requires:

$$C_c\dot{p}_c = Q_d - Q_c - V_{c_h}(h,\theta)\dot{h} - V_{c_\theta}(h,\theta)\dot{\theta}, \qquad (5)$$

where C_c is the cushion capacitance given by

$$C_c = V_c(h,\theta)/\rho a^2 \qquad (6)$$

V_c is the cushion volume,
ρ is the air density,
Q_d is the volume flow of air in the duct,
Q_c is the exit flow out of the cushion,
and V_{c_h} and V_{c_θ} are the partial derivatives of V_c with respect to h and θ respectively.

The lumped inertance equation for the duct:

$$(\frac{\rho L_d}{A_d})\dot{Q}_d = \Delta p_f - p_c - (\frac{4fL_d}{d})(\frac{\rho Q|Q|}{2A_d^2}) \qquad (7)$$

where L_d is the duct length,
A_d is the duct cross-sectional area,
Δp_f is the static pressure rise across the fan,
d is the duct diameter or equivalent diameter,
and f is the British duct friction factor.

The description is completed with the steady fan law,

$$\Delta p_f = p_0 + p_0 Q_d + p_2 Q_d^2 + p_3 Q_d^3 + p_4 Q_d^4 \qquad (8)$$

and the exit flow law,

$$Q_c = C_D a_\ell(h,\theta)(\frac{2p_c}{\rho})^{1/2} \qquad (9)$$

where C_D is the exit discharge coefficient, and
a_ℓ is the cushion leak or air escape area.

Equations 8 and 9 apply at each instant of time.

When the capacitance and inertance are negligible the system is fourth order and the lumped capacitance and inertance equations become

$$Q_c = Q_d - V_{c_h}(h,\theta)\dot{h} - V_{c_\theta}(h,\theta)\dot{\theta} \qquad (10)$$

and

$$\Delta p_f = p_c + (\frac{4fL_d}{d})(\frac{\rho Q_d|Q_d|}{2A_d^2}) \qquad (11)$$

respectively.

With the exit flow equation, (9), these provide the boundary conditions for equations 1 and 2.

GEOMETRIC FUNCTION APPROXIMATIONS

Four terms in the above equations are geometry dependent; these are the geometric functions $a_\ell(h,\theta)$, $a_f(h,\theta)$, $V_c(h,\theta)$, and $\bar{x}(h,\theta)$. The calculation of these functions is facilitated by making two initial approximations. First, the curved edges at the lip of the skirt are replaced with a simple mean perimeter line. Second, the flow area associated with the rounded tips of the segments is modelled as an equivalent leak height which is calculated using the above perimeter, the measured flow, and the cushion pressure when all the segment lower tips are just touching the ground. This leak height is indicated as H_L in

figure 3, which also shows the three geometry cases in which each of the functions must be calculated. The three cases are:

i) the skirt is totally out of contact with the ground,

ii) the skirt is in partial contact with the ground, that is, the plane formed and bounded by the undeformed skirt lip perimeter and the ground plane intersect,

and

iii) the skirt is in contact with the ground throughout its entire perimeter.

The details of the geometry are complex and tedious [11] and are not presented here, however some discussion is appropriate since the nature of assumptions made about the shape of the footprint will be shown to have a significant effect on cushion operation.

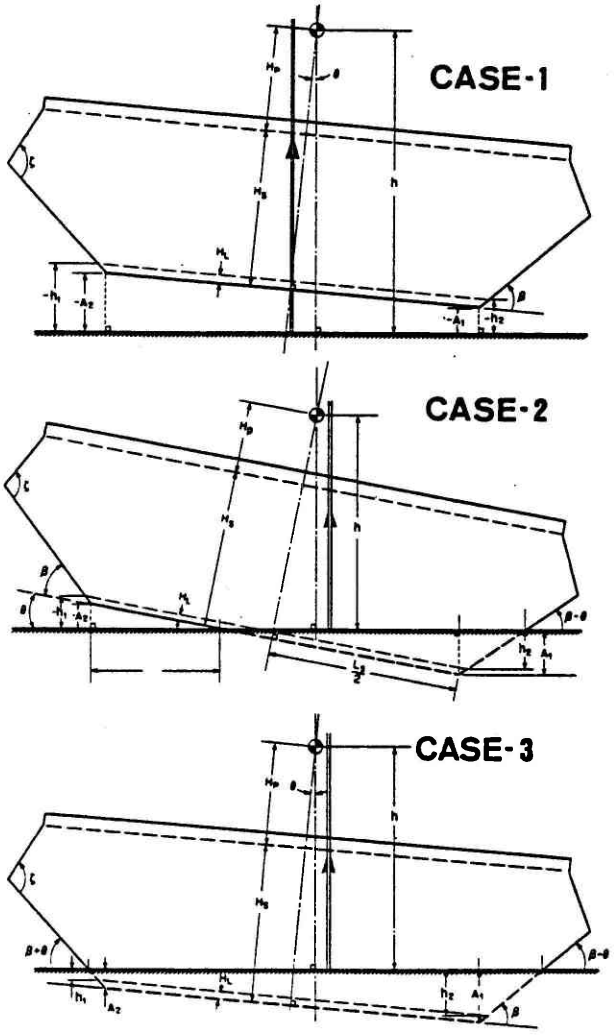

FIGURE 3: Side View of Cushion for the Three Geometry Cases

The detailed footprint area used in the three cases is shown in figure 4 and has the dimensions given in the first column of table 1. These dimensions are those of the UTIAS laboratory test facility hereafter referred to as the Labrig. Another approximation, referred to here as the "alternate" footprint, has been constructed. This footprint is the same as the detailed area except that the corner radius, Rs, is assumed to be zero

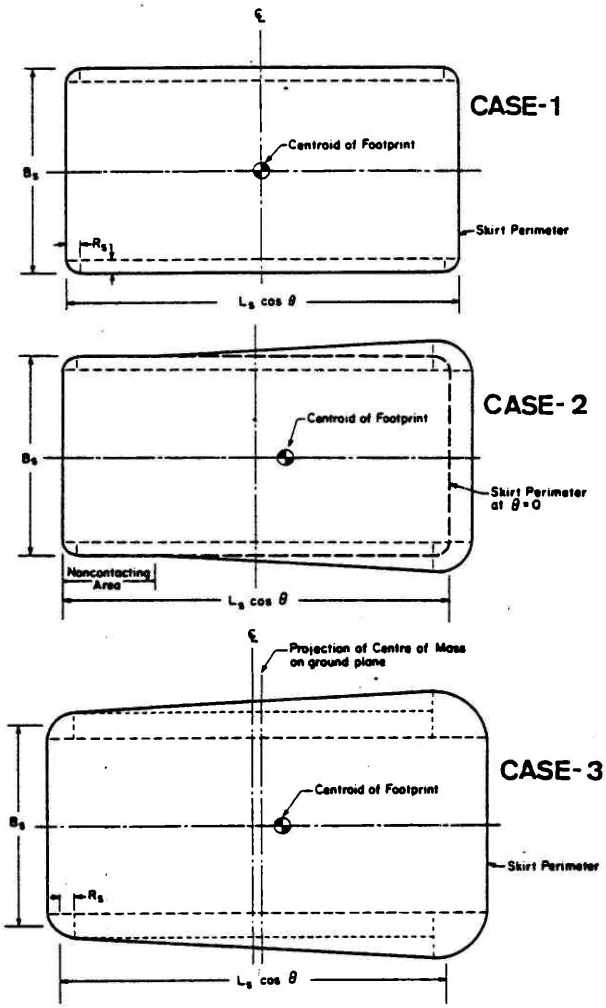

FIGURE 4: Detailed Footprint Shape for the Three Geometry Cases

TABLE 1

Footprint Details

	Detailed Footprint	Alternate Footprint	Rectangular Footprint	x20 Scaled Vehicle
Ls (m)	2.214	2.214	2.214	44.280
Bs (m)	0.991	0.991	0.991	19.820
Rs (m)	0.326	0.000	0.000	6.520
β (deg)	32.5	32.5	32.5	32.5
m (kg)	97.7	97.7	97.7	780000

so that the case 1 footprint is a rectangle. Column 2 of table 1 gives the appropriate dimensions. A simpler footprint is obtained by assuming Rs=0 and that the footprint does not expand laterally as a result of ground contact during pitch motion. Thus the side triangles and curved section of cases 2 and 3 are ignored and a rectangular footprint is obtained. Of the three footprints the detailed footprint most closely duplicates tracings made of the footprint periphery of the Labrig test cushion.

In the results that follow all of the geometry functions are affected by the changes in footprint except the cushion volume. $V_c(h,\theta)$ is calculated assuming that Rs=0 and is similar to the alternate footprint except that the lower corner areas are formed by extension of the side triangle perimeter lines to meet the line formed by the outer edge of the skirt ground contact area at the lower end. Thus the lower ellipsoidal corners are replaced with trapezoids. The hysteresis functions, $H_h(h,\theta,\dot{h},\dot{\theta})$, and $H_p(h,\theta,\dot{h},\dot{\theta})$, are altered by the change in Rs. The associated forces are larger for a given (h,θ) when Rs=0 since the cushion perimeter length is increased over the detailed perimeter. The change in footprint area couples with associated changes in $\bar{x}(h,\theta)$ to produce changes in the restoring moment. The air leakage area, $a_\ell(h,\theta)$, is larger for a given (h,θ) when Rs=0. The geometry function differences are summarized in table 2 where geometry functions which are identical for different footprints have been marked in the appropriate column.

SIMULATION RESULTS AND DISCUSSION

Static simulation results were obtained with the skirt hysteresis set to zero. Figure 5 gives experimental static pitch stiffness results along with theory for the three different footprint approximations of the Labrig test model. When compared to the measured values, the rectangular footprint underestimates the stiffness by 27%, the alternate footprint overestimates the stiffness by 24%, while the detailed area overestimates by 2.5%. Measured values of footprint area are presented with predictions of the three footprint approximations are shown in figure 6. Note that when Rs=0, the footprint areas at $\theta = 0$ are overestimated by about 5.5% compared to 1.8% for the detailed area. At larger pitch angles, above 2.5 degrees, the rectangular area underestimates the measured area. The alternate and detailed footprints continue to overestimate the area, at θ=3.2° the alternate is 16% over and the detailed is 7.0% over. The slope of the footprint area curve is important as it influences the dynamic motion through the pitch stiffness. Thus, although the rectangular footprint gives a closer fit to the footprint area on average the detailed area gives a preferable representation of these geometry related parameters.

Both the footprint area and restoring moment functions depend on the segment angle, β, shown in figure 1. The angle used in all theory presented here is 32.5°; this value was obtained from direct measurements of the angle between the tangent to the outer edge of the segment near its tip, and

TABLE 2

Correspondence of Cushion Geometry Functions

Geometry Function	Detailed Area	Alternate Area	Rectangular Area	Comments
$a_\ell(h,\theta)$		Function is the same for alternate and rectangular footprints.		Modified by change in Rs
$a_f(h,\rho)$				
$M_p(h,\theta)$				
$V_c(h,\theta)$	Function is the same for all footprints.			Obtained in separate unaffected calculation.
$H_h(h,\theta,\dot{h},\dot{\theta})$		Function is the same for alternate and rectangular footprints.		Modified by change in Rs
$H_p(h,\theta,\dot{h},\dot{\theta})$		Function is the same for alternate and rectangular footprints.		Modified by change in Rs

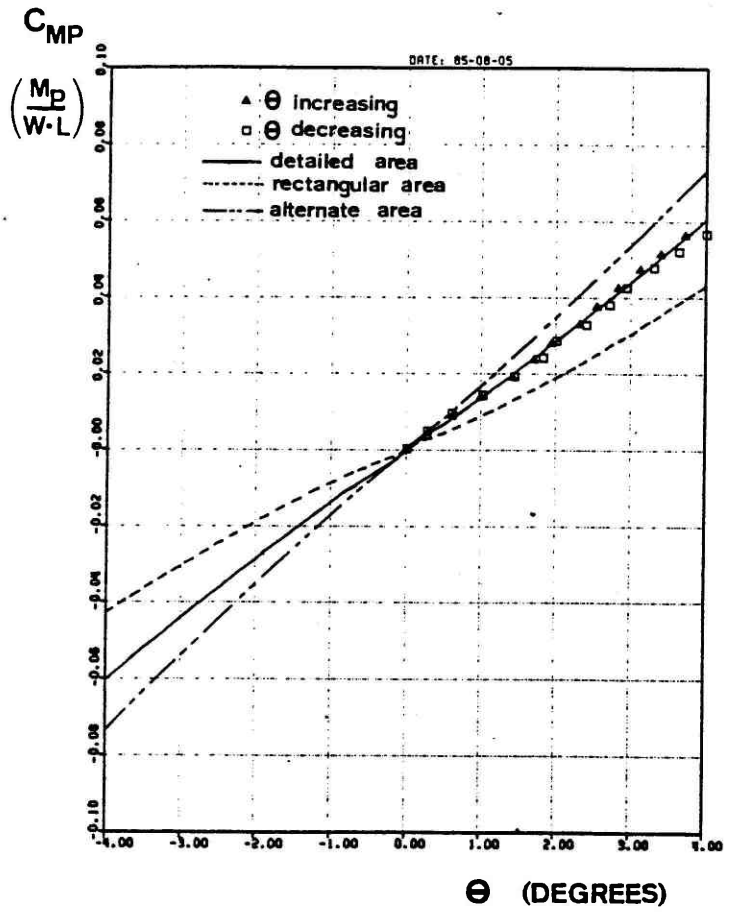

FIGURE 5: Pitch Stiffness - Experimental Results and Theory for Three Footprint Area Approximations
a) Detailed Area, b) Rectangular Area, c) Alternate Area

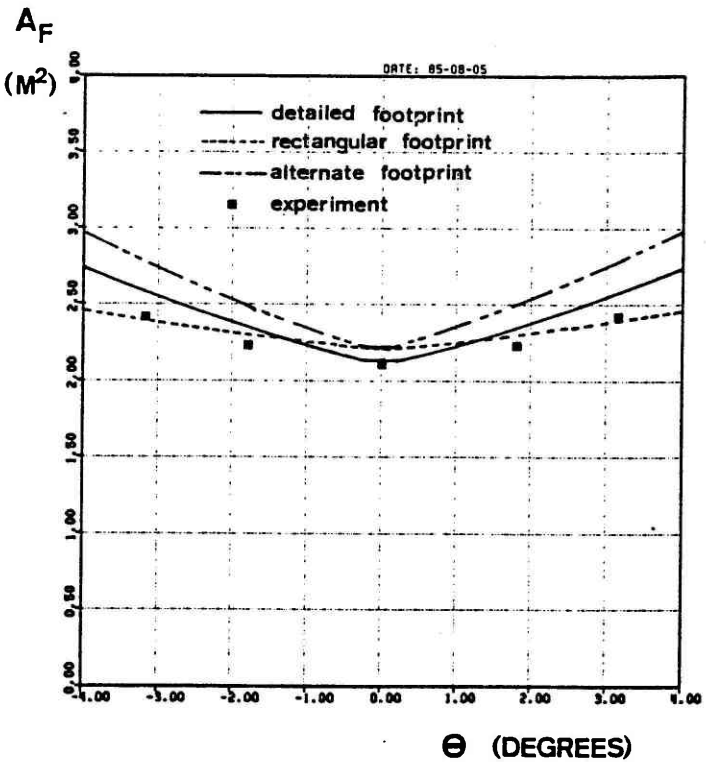

FIGURE 6: Footprint Area - Experimental Results and Theoretical Results for Different Footprint Approximations
a) Detailed Area, b) Rectangular Area, c) Alternate Area

the ground plane. This was necessary because cushion pressure caused significant curvature of the segment outer surface between the knee and tip. Measurements of the distances from the segment knee to ground and from the segment tip to the perpendicular from the ground to the knee gave the design value of 40° for β. Still another estimate of β was obtained by determining the angle for which the detailed area gave the best fit to the area data: this value was 38°. If 38 or 40° is used in the theory the following changes occur in the results. The pitch stiffness is reduced in all cases so that the alternate area curve now agrees closely with the measured values, and the detailed area stiffness curve lies closer to the rectangular curve of figure 5. The footprint area predicted by the detailed geometry agrees with the footprint data closely while the alternate footprint still overestimates at all angles. The results for the rectangular area greatly underestimate the pitch stiffness and show only a very small footprint area change during pitch motion. The discrepancy between the moment and area suggests that there are forces which produce moment on the cushion not included in the analysis. Current speculation is that these forces are produced by the air supply ducts and/or an elastic force resulting from skirt ground contact.

All dynamics simulation results are presented for cushions with β of 32.5° and are the response to a simple initial disturbance test. The model is clamped in equlibrium at 2° pitch until t=0 when the vehicle is released and the response is plotted. The fourth order system model is used with the three footprint area approximations to obtain the comparative results shown in figure 7. The pitch and heave responses are given for each approximation. Of the three, the rectangular skirt is much more highly damped.

This increase in damping may be interpreted by loose analogy with a second order system with viscous damping as follows. Make the gross, and for pitch angles over 0.25 to 0.5° unfounded, assumption that the pitch and heave motions are uncoupled, so that each is represented by an equation of the form

$$\ddot{z} + 2\zeta\omega_n\dot{z} + \omega_n{}^2 z = 0 \qquad (12)$$

where ζ is the damping ratio $=0.5C/(mk)^{1/2}$
C is the viscous damping coefficient
m is the mass or pitch moment of inertia
k is the heave or pitch stiffness
and ω_n is the natural frequency $= (k/m)^{1/2}$.
The geometry details of table 1 and the function comparisons of table 2 indicate that near θ = 0 where the footprint areas, leak areas, and heave heights will be close, the main difference between the rectangular and alternate footprints is the slope of the moment curve indicated in figure 5. The hysteretic damping energy loss per cycle can be represented by an equivalent viscous dashpot. The value of this dashpot will be close for the alternate and rectangular footprints since the hysteresis forces are determined by the same

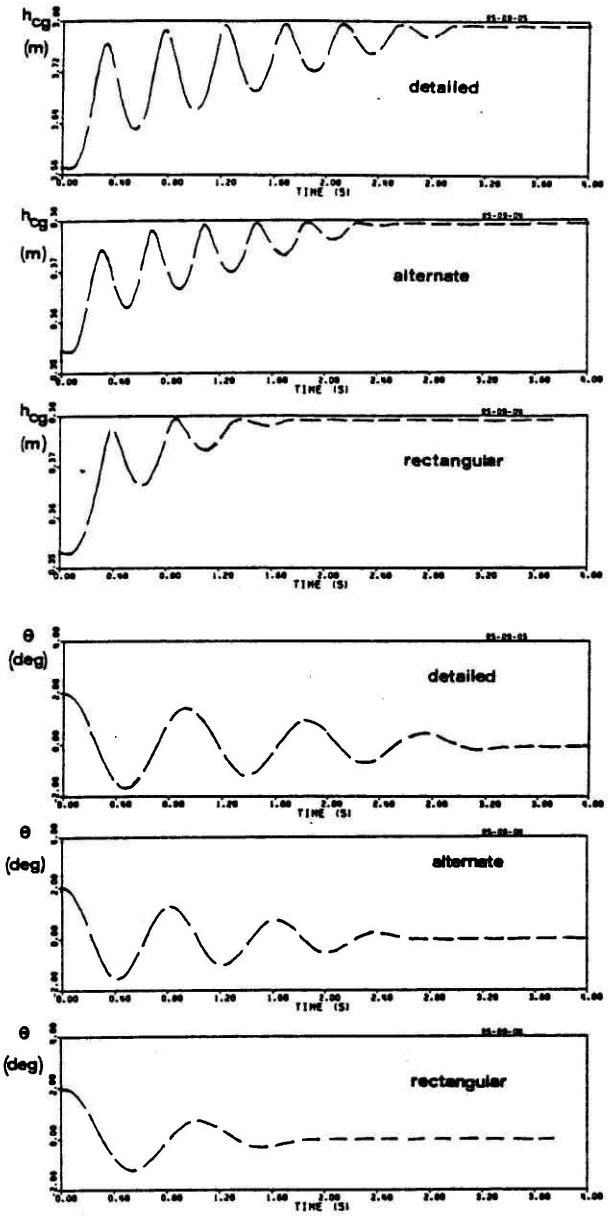

FIGURE 7: Initial Disturbance Response for Three Footprint Approximations
a) Detailed Area, b) Rectangular Area, c) Alternate Area

function of h and θ and near θ = 0 the heave height will be close. Thus the decrease in stiffness seen with the rectangular footprint leads to an increased damping ratio, ζ. This stiffness change is further evidenced by the reduction in pitch frequency which can be seen by comparing the number of cycles complete at t = 1.2s on the lower two curves of figure 7. Similarly the rate of change of footprint area with respect to heave height is smaller in magnitude at non-zero pitch angles so that the heave stiffness of the rectangular footprint is reduced and that ζ is increased in heave as well.

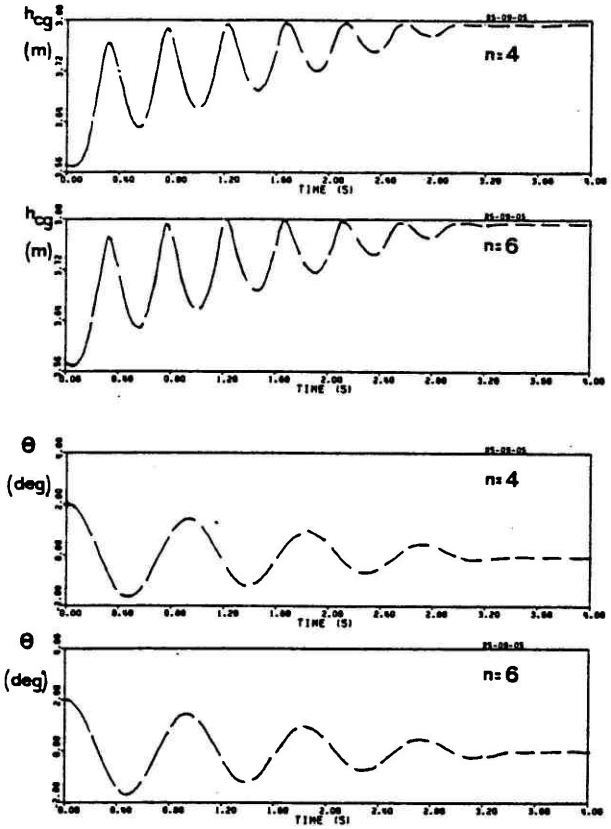

FIGURE 8: Response of the Fourth and Sixth Order Models To a Two Degree Initial Condition Disturbance in Pitch - Labrig Model

Further evidence of this is again shown by the decrease in frequency of the rectangular footprint heave motion from that of the alternate footprint. Differences between the detailed geometry and the alternate geometry are more subtle. Although the frequency change follows from the differences in the two stiffnesses the damping factor is seen to be only slightly different. This results from the coincident reduction of damping and stiffness of the detailed area compared to the alternate area.

Figure 8 shows the responses predicted under the detailed area assumptions for the fourth and sixth order models of craft dynamics. As can be seen there is virtually no difference in the response. Similar simulations are shown in figure 9 for a craft geometrically scaled to 20 times the size of Labrig. The importance of the additional orders is indicated by the large difference in the response predicted by the two models. This is especially significant since the frequencies involved are low, about 0.65 Hz in heave and 0.33 Hz in pitch. The large difference in response is mainly due to capacitance since the fan characteristic closely follows the steady fan characteristic. Although the dimensions of this craft place it slightly outside the range of lumped parameter applicability given in equation 1 the assumption is expected to be quite good. This is because the inertance effects are small and Hinchey [12] has shown that wave propagation effects are small in cushions of this size if feed

holes are located peripherally, as is commonly the case with ACV's.

The amount of hysteresis used in the simulations was chosen in an ad hoc fashion since no reliable measurements are currently available. In particular, the hysteresis force per unit length chosen for the scaled up version was selected so that a lightly damped oscillation was produced when the sixth order model was used. With the fourth order model this amount of hysteresis gives the well damped response shown in figure 9. Similarly when hysteresis was scaled to the Labrig model of the well damped response of figure 10 was obtained. Note the close correspondence of this response to that of the fourth order model of the ×20 scaled-up vehicle. Also this scaled hysteresis is 12 times that used to obtain the responses in figures 6 to 8. The amount of hysteresis selected for the ×20 scaled-up version was 0.18% of the vehicle weight per metre of skirt. This is an extremely large value and is not likely feasible in a flexible skirt design.

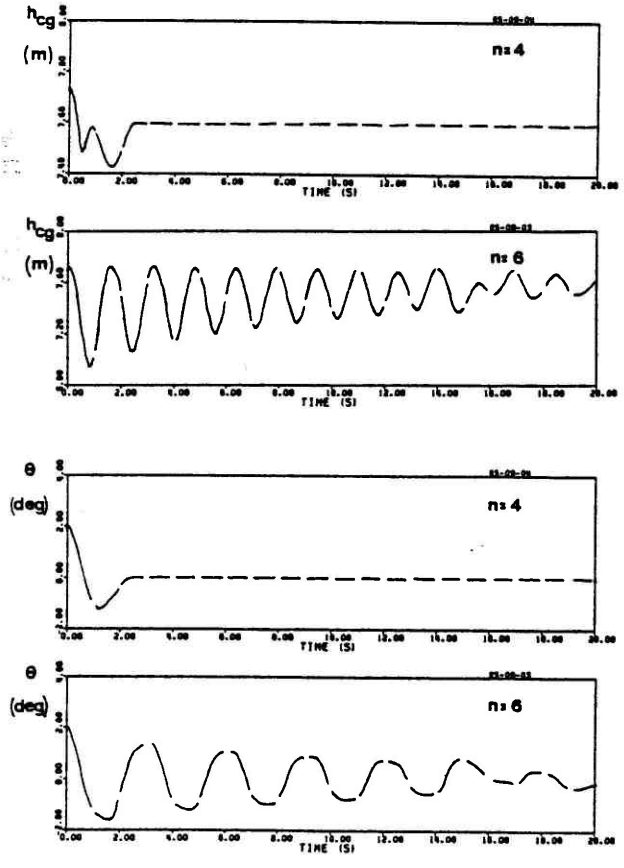

FIGURE 9: Response of the Fourth and Sixth Order Models to a Two Degree Initial Condition Disturbance in Pitch - x20 Scale-up of Labrig Model

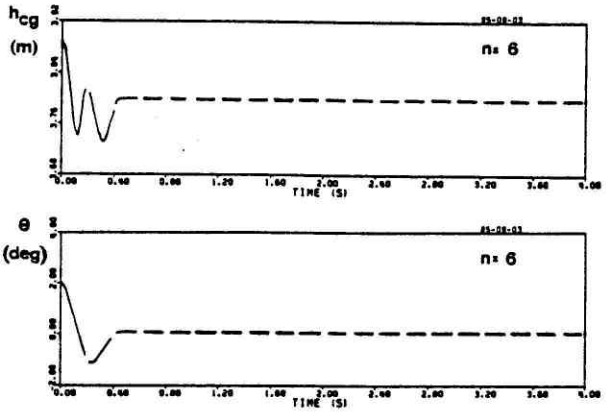

FIGURE 10: Response of Labrig Model to a Two Degree Initial Condition Disturbance in Pitch - Damping is Scaled from the x20 Scale-up Response

CONCLUSIONS

Several important factors affecting the response of the nonlinear segmented skirt model have been determined. In particular, the choice of the footprint shape approximation has surprisingly large effects on the predicted vehicle static and dynamic behaviour. A fairly high degree of geometry detail is required to get accuracy within 10 to 20 percent for major vehicle response parameters, for example, pitch stiffness. Although cushion capacitance and duct inertia have almost no effect on pitch heave dynamics for the laboratory scale model the ×20 scaled-up simulations indicate large changes associated with these orders. These results suggest that in an uncompartmented air cushion the skirt materials normally used will not provide adequate damping for a large scale craft. Hence designers planning to build larger craft with this skirt system should give careful consideration towards ensuring that the craft has adequate damping.

NOMENCLATURE

a	speed of sound in air
a_f	cushion footprint area
a_ℓ	cushion air escape or leakage area
A_d	duct cross-sectional area
Bs	cushion width at bottom of skirt
C	viscous damping coefficient
C_c	cushion pneumatic capaciance
C_D	discharge coefficient
C_{MP}	pitch moment coefficient
d	duct diameter or equivalent diameter
f	friction factor
f	frequency
g	gravitational acceleration
h	height of centre of mass above datum
H_h	heave hysteresis force
H_p	pitch hysteresis moment
I_{yy}	moment of inertia in pitch
k	stiffness

L length in general, length of craft hard structure
L_d duct length
L_s cushion length at bottom of skirt
m mass, mass of cushion
M_p total restoring moment
M_{p_f} portion of restoring moment due to momentum flux of air from cushion
p_c cushion pressure
Δp_f static pressure rise across fan
Q_c exit air flow from the cushion
Q_d volume flow of air in the duct
R_s radius of cushion corners at skirt bottom
t time
V_c cushion volume
W craft all-up weight
x variable
$\bar{x}$ moment arm of centre of pressure
β segment angle with ground when $\theta = 0$
ζ damping factor
θ pitch angle
π 3.14159...
ρ air density
ω_n natural frequency (rad/s)

ACKNOWLEDGEMENTS

This project was made possible by the substantial support of two Canadian Government agencies, Transport Canada's Transportation Development Centre (TDC) and the Natural Sciences and Engineering Research Council. The support of Mr. J. E. Laframboise of TDC is gratefully acknowledged.

REFERENCES

1) Graham, T. A., Sullivan, P. A., Hinchey, M. J., HEAVE STIFFNESS MEASUREMENTS ON A LARGE SCALE AIR CUSHION, Seventeenth Canadian Symposium on Air Cushion Technology Preprints, Ottawa Canada, Oct. 1983.

2) Sullivan, P. A., Hinchey, M. J., et al, RESEARCH INTO AIR CUSHION STABILITY: 1979 REPORT, Transportation Development Centre Transport Canada, TP3109E, TDC File: D500-431-1, January 1982.

3) Sullivan, P. A., Hartmann, P. V., Graham, T. A., APPLICATION OF SYSTEM IDENTIFICATION FLIGHT ANALYSIS TECHNIQUES TO THE PITCH-HEAVE DYNAMICS OF AN AIR CUSHION VEHICLE, CASI Journal Transactions, Vol. 29, No. 4, December 1983.

4) Wylie, E. B., Streeter, V. L., FLUID TRANSIENTS, FEB Press, Corrected Edition 1983.

5) Sweet, L. M., Richardson, H. H., and Wormley, D. N., LINEARIZED MODELS, STABILITY CRITERIA AND EXPERIMENTAL VERIFICATION FOR PLENUM AIR CUSHIONS WITH COMPRESSOR-DUCT INTERACTIONS, DOT-FRA-ORD & D74-40, Department of Transportation USA, May 1974.

6) Hinchey, M. J., HEAVE INSTABILITIES OF AMPHIBIOUS AIR CUSHION SUSPENSION SYSTEMS, UTIAS Report No. 246, Nov. 1980.

7) Boghani, A. B., Captain, K. M., and Wormley, D. N., HEAVE-PITCH -ROLL ANALYSIS AND TESTING OF AIR CUSHION LANDING SYSTEMS, NASA CR-2917, 1978.

8) Doctors, L. J., THE EFFECT OF AIR COMPRESSIBILITY ON THE NONLINEAR MOTION OF AN AIR CUSHION VEHICLE OVER WAVES, I. Mech. E, 1977.

9) Doctors, L. J., NONLINEAR MOTION OF AN AIR CUSHION VEHICLE OVER WAVES, Journal of Hydronautics, Vol. 9, No. 2, April 1975.

10) Swift, M. R., Lebel, D., HEAVE MOTION OF AIR CUSHION VEHICLES, Journal of Hydronautics, Vol. 12, No. 2, April 1978.

11) Sullivan, P. A., et al, INVESTIGATIONS OF THE DYNAMICS OF LARGE SCALE AIR CUSHIONS, Transportation Development Centre, Transport Canada, Contract Report (in preparation).

12) Hinchey,M. J., Sullivan, P. A., and Dupuis, A., ON THE HEAVE DYNAMICS OF LARGE AIR CUSHION PLATFORMS, Journal of Sound and Vibration, Vol. 96, No. 4, pp 469-484, 1984.